Astron. Astrophys. 214, 227–238 (1989)

ASTRONOMY AND ASTROPHYSICS

Rotational modulation and flares on RS Canum Venaticorum and BY Draconis stars

XII. Near-to-simultaneous high resolution UV and optical observations of II Pegasi during July 1984

P. B. Byrne [1], P. Panagi [1], J. G. Doyle [1], C. A. Englebrecht [2], R. McMahan [3], F. Marang [2], and G. Wegner [3]

[1] Armagh Observatory, Armagh BT61 9DG, Northern Ireland
[2] South African Astronomical Observatory, P.O. Box 9, Observatory 7935, South Africa
[3] Department of Physics and Astronomy, Dartmouth College, Hanover, NH 03755, USA

Received October 26, 1987; accepted August 26, 1988

Summary. Near-to-simultaneous high resolution ground-based optical and IUE satellite-ultraviolet spectroscopy of the RS CVn star II Peg are presented along with a contemporaneous optical light curve. Using these we show that II Peg's chromospheric and transition region radiative losses in July 1984 are lower than the means recorded in previous years, although individual comparably low values have previously been reported. Our high resolution IUE spectra allow us to estimate the flux in the Ly α line for the first time in this star and to show that it is at least comparable to the combined flux of the principal optical and other UV emission lines. Furthermore, there is evidence of variability in all of the emission lines which appears to be correlated with the optical spots. This correlation is more complicated than a simple rotational modulation however. Equivalent widths of selected TiO bands confirm a change in mean photospheric effective temperature with phase suggested by changes in broadband $(V-I)_{KC}$ colour. Line profiles were obtained at two rotational phases for the principal UV emission lines. They show a clear excess broadening over and above the combined instrumental plus Doppler broadening. We show that the Hα profile is complex and variable in time but that the time sequence of profiles obtained may be interpreted in terms of a feature crossing the disk of II Peg. The Ly α profile is asymmetric with respect to the stellar rest frame in the same sense as Hα but shows no detailed correlation. We have examined two published radial velocity curves and find that one (Vogt, 1981) clearly fits the present data better.

Key words: stellar atmospheres – RS CVn binaries – IUE spectra – starspots and plages

1. Introduction

It is well established that the wave-like variations in the optical light curves of rapidly rotating late-type stars, in particular the RS CVn and BY Dra variables, can be interpreted in terms of cool surface spots analogous to sunspots (see e.g. reviews by Vogt, 1983, and Rodonò, 1986). Associated with the modulation of optical light are variations in the strengths of chromospheric and transition region emission lines which are generally in antiphase with the optical light curve (Rodonò et al., 1986, 1987; Papers I and III in this series). This is consistent with a solar-like model in which magnetic structures overlying the photospheric spots give rise to excess heating of the outer atmosphere (Byrne et al., 1987; Paper VI).

All aspects of the behaviour of these objects are highly variable on many time scales. Furthermore this activity manifests itself over a wide range of wavelengths, each giving information on a different temperature regime within the atmosphere, from the cool photospheric spots to the multi-million degree corona. For these reasons it is important where possible to obtain observations in different parts of the electronmagnetic spectrum, as near to simultaneous as possible.

In this paper we describe almost simultaneous satellite UV and ground-based optical spectroscopy as well as contemporaneous broadband optical photometry of the RS CVn system II Peg. II Peg is in many ways a typical RS CVn system. It is a 6.72 day period spectroscopic binary. The orbital and spot wave periods are almost identical. The active star, itself a K2 subgiant, has a low mass companion which has never been detected in the spectrum. This makes analysis of II Peg's spectrum relatively simple compared with other RS CVn systems, since there are no line blending problems. A fuller discussion of the observational history of II Peg will be found in Paper I and so will not be repeated here.

In an earlier paper (Paper III) we detected a discrete region on II Peg whose emission in transition region lines was at least a factor of five greater than that of the general stellar surface. This region coincided closely in stellar longitude with the dominant optical spot. Paper VI analysed the physical characteristics of this discrete emitting region and showed that it could be interpreted in terms of a complex of large but solar-like magnetic loops.

Andrews et al. (1988, Paper IX) described follow-on IUE spectroscopy and optical photometry of II Peg in 1983. Their data, covering only part of a stellar rotation, showed only a weak signature of rotational modulation. From their data the discrete emitting region detected in 1981 appears to be absent. Nevertheless, they did observe UV flares lasting several hours whose

Send offprint requests to: P. B. Byrne

* Based in part on observations collected with IUE at the ESA Satellite Tracking Station, Villafranca (Spain) and with the Isaac Newton telescope, operated by the Royal Greenwich Observatory at the Observatorio del Roque de los Muchachos on La Palma (Canary Islands)

physical conditions closely resembled those of the region observed in 1981 (Doyle et al., 1989).

Our main objective in the present work was (1) to use near-to-simultaneous high resolution UV and optical spectra to search for evidence of discrete surface features from the photosphere, through the chromosphere and into the transition region and, (2) by comparing our results with those obtained previously, to examine the evolution of II Peg's activity in time. Provision of contemporaneous photometry would also allow comparison of any results with the spot distribution at that epoch.

Section 2 presents the data. In Sect. 3 we derive a spotmodel based on the optical broadband photometry and show that the strengths of TiO bands change with phase. Section 4 examines the chromospheric and transition region line fluxes and their dependence on spot visibility while Sect. 5 discusses the profiles of these lines. We use our optical and ultraviolet data to examine two previously published radial velocity curves in Sect. 6. Section 7 conducts a general discussion on the results and our conclusions are summarized in Sect. 8.

2. Observations and data reduction

2.1. Photometry

The photometric observations were taken by two of us (C.E. and F.M.) on the 0.5 m telescope at the South African Astronomical Observatory (SAAO) at Sutherland, on six nights during the period July to September 1984. Transformations to the $UBV(RI)_{KC}$ (Kron-Cousins) system were achieved by reference to E-region standard stars (Menzies et al., 1980). The resulting magnitudes and colours will be found in Table 1.

To improve the coverage of the light curve this dataset was supplemented by data already published in the literature. Kaluzny (1984) gives Johnson *UBV* photometry of II Peg taken during a two week period in mid-August 1984, while Arevalo et al. (1985) give differential *UBVRI* photometry covering a one month period from mid-August. On comparing the three data sets we find that the data of Arevalo et al. appears much more scattered than the others, in spite of a detailed overlap with Kaluzny. For this reason we have preferred to use the latter dataset. Figure 1 shows the light curve for II Peg resulting from phasing our SAAO data and Kaluzny's according to the epoch given by Raveendran et al. (1981). There is a seriously discrepant point at phase 0.65 in the SAAO data with respect to that of Kaluzny. We have been unable to reconcile this difference and have omitted the point ringed in Fig. 1 from further consideration.

The *V* light curve given in Fig. 1 exhibits an asymmetric wave, typical of RS CVn stars, with primary minimum at about phase, $\varphi \approx 0.3$–0.4 and some indication of a secondary minimum at about phase, $\varphi \approx 0.6$–0.7. This would indicate the presence of at least two centres of spot activity separated by about $\Delta\varphi \approx 0.4$ or 140° in longitude. The total amplitude of the variation, $\Delta V \approx 0.12$, is typical for II Peg and indicates a substantial, non-uniform surface coverage by spots.

The $(B-V)$ colour exhibits no obvious variation with phase, although there is a slight tendency to reddening near the phase of light curve minimum. We also remark on the unusually large scatter in this colour, which could indicate the presence of low-level flaring activity in the B band. The mean $(B-V)$ is $\approx +1.00$. $(V-I)_{KC}$ however does show signs of a low amplitude modulation with phase, consistent with this colour being reddest at the phase of maximum spot visibility.

Table 1. SAAO photometry of II Peg. Phases, φ, have been calculated according to the ephemeris of Raveendran et al. (1981) ($JD_0 = 2443030.396$, $P = 6.724464$ day)

HJD	Phase	V	$(B-V)$	$(V-I)_{KC}$
2445892.63915	0.646	7.618	1.064	1.258
2445896.63472	0.240	7.617	1.035	1.254
2445922.59477	0.101	7.526	1.028	1.224
2445923.56004	0.244	7.604	1.036	1.246
2445924.55574	0.392	7.623	1.031	1.263
2445928.54857	0.986	7.484	1.004	1.239

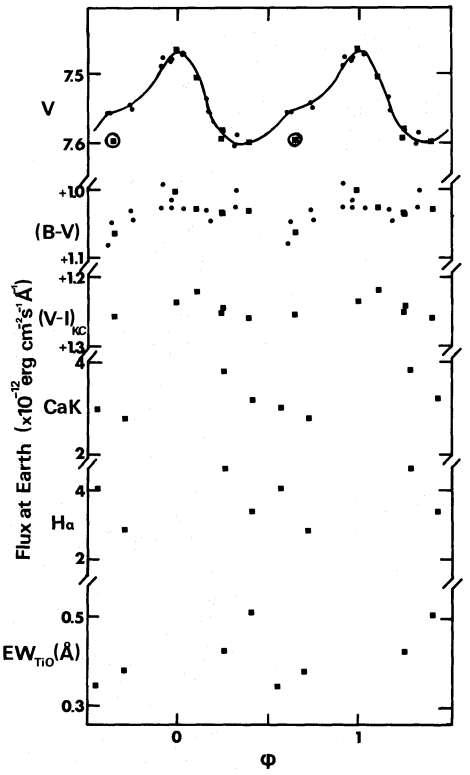

Fig. 1. Optical and near-IR light curves for II Peg in mid-1984. The ringed point in the *V* light curve is explained in the text. The solid curve is a two-spot model fitted to the data. The bottom panel shows the sum of the equivalent widths relative to a locally defined continuum of two TiO bands in the Hα spectral region as a function of phase

2.2. Optical spectroscopy

The optical spectroscopy was carried out by Dr. J.V. Wall as service observing on the 2.5 m Isaac Newton Telescope (INT) at the Observatorio del Roque de los Muchachos of the Astrophysical Institute of the Canary Islands. The telescope was equipped with the Cassegrain Intermediate Dispersion Spectrograph (IDS) and the Image Photon Counting System (IPCS) detector. Observations were made on four consecutive nights, 15th to 18th July 1984 inclusive. On each of the first three nights, four spectra were obtained centred on ≈3950 Å, ≈6260 Å, ≈6560 Å, and ≈6820 Å. Only two spectra were secured on the last night, one each in the first and third spectral ranges. Each spectrum covered a range of

Table 2. Details of optical and UV spectra and the corresponding emission line fluxes at Earth derived from them. Phases, φ, have been calculated according to the ephemeris of Raveendran et al. (1981) ($JD_0 = 2443030.396$, $P = 6.724464$ day). Interstellar absorption has been removed in Mg II and Ly α and also geocoronal emission in Ly α

HJD (mid-exp.) JD 2445800+	φ	λ_c	Line fluxes at Earth (10^{-13} erg cm^{-2} s^{-1})				
			Ca II H	Ca II K	Hε	Hα	EW (Hα)
96.70700	0.251	3950	36.4	37.8	10.5	–	–
96.74109	0.256	6563	–	–	–	46.1	1.39 Å
96.76021	0.259	6275	–	–	–	–	–
96.77817	0.261	6825	–	–	–	–	–
97.69694	0.398	3950	30.2	31.5	6.4	–	–
97.71931	0.401	6563	–	–	–	33.6	0.83 Å
97.73512	0.404	6275	–	–	–	–	–
97.74939	0.406	6825	–	–	–	–	–
98.74655	0.554	3950	29.1	29.7	6.1	–	–
98.76537	0.557	6563	–	–	–	40.2	1.10 Å
98.77839	0.559	6825	–	–	–	–	–
98.78917	0.560	6275	–	–	–	–	–
99.75895	0.705	3950	27.3	27.5	6.1	–	–
99.77803	0.707	6563	–	–	–	28.3	0.69 Å

HJD (mid-exp.) 2445800+	φ	IUE Image No.	Exp. (min)	Line fluxes at Earth (10^{-13} erg cm^{-2} s^{-1})	
				Mg II h	Mg II k
96.34482	0.197	LWP 3760	20	29.2	37.2
99.33535	0.642	LWP 3791	30	31.2	40.2

				Ly α	O I[a]	C II[a]	C IV[a]	He II	Si II[a]
96.48719	0.218	SWP 23465	376	160	–	2.9 –	5.8 –	4.3	1.0 0.9 0.3
99.48328	0.664	SWP 23473	386	160	2.1 2.8 2.3	3.5 3.3	4.8 1.9	2.9	0.8 0.9 0.2

[a] The multiple entries are for the individual members of the multiplet where these are measurable

wavelength of ± 100 Å. Thus the Ca II H and K and Hα emission lines were recorded once per night. CuAr arc spectra were taken with each observation to ensure a reliable wavelength calibration. Subsequent fitting of the arc lines indicated that the resolution (FWHM) of the spectra was better than 0.2 Å in all cases. Table 2 summarizes the times of observation and the phases to which they correspond. The sequence begins preceding, but close to, light curve minimum and ends about maximum. Unfortunately no spectra of flux standards were obtained due to restricted observing time.

Initial reduction and wavelength calibration of the optical spectra were performed using standard procedures within the SPICA suite of routines available on the UK STARLINK astronomical computing network (Bromage, 1984). Removal of the wavelength dependence of the detection system in the resulting spectra was achieved by reference to a flux calibrated spectrum of the K0 III star, SAO 55164, provided by the World Data Centre databank at the NASA Goddard Space Flight Centre. In order to establish a flux scale the spectrum was then multiplied by a scaling factor to account for the difference in magnitude between II Peg and the standard star in the photometric band closest to the spectral region under consideration (e.g. the *R* band magnitudes were used to calibrate the red spectral bands). This scaling factor was deduced from the multi-colour light curve data presented in Table 1. Examples of the spectra in the vicinity of Hα and Ca II H and K are given in Fig. 2. Ca II H and K, Hε, and Hα are all seen strongly in emission in our spectra.

2.3. *UV spectroscopy*

High dispersion ultraviolet observations were also obtained by one of us (JGD), using the International Ultraviolet Explorer (IUE) satellite on the first and last of the above four nights. These yielded spectra preceding light curve minimum by $\Delta\varphi \approx 0.1$ and the other just before maximum. One exposure was taken in each of IUE's long wavelength ($\approx$1900–3100 Å) and short wavelength ($\approx$1150–1950 Å) cameras, principally to expose for the Ly α and Mg II h and k emission lines. The resolution of IUE is given as $\approx$0.07 Å for Ly α and $\approx$0.17 Å for Mg II h and k by Bianchi et al. (1981). Details of the IUE spectra are also summarized in Table 2.

All reductions were performed within the IUEDR (Giddings, 1983a) and DIPSO (Howarth and Masdlen, 1983) facilities

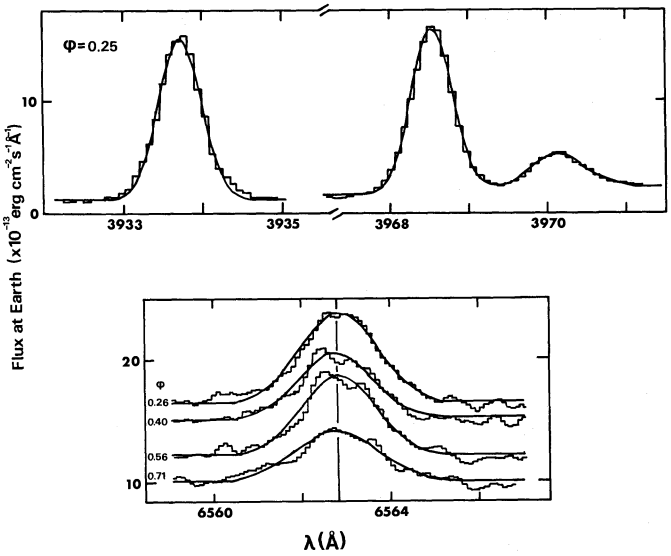

Fig. 2. Ca II H and K and the Hε (upper panel) profiles on the first night of INT observation and the Hα profiles (lower panel) on all four nights. The Hα profiles have been displaced vertically on successive nights to make the diagram easier to read. The continuous curves are the gaussian fits referred to in the text

available on the STARLINK computer network. At the outset the raw data, which consists of a two-dimensional image of the echellogramme, were displayed on a greyscale image display terminal and any bright points due to extraneous events, such as cosmic rays, were identified and flagged so that the subsequent extraction took them into account. Considerable care was taken at this stage since the spectra, apart from Ly α and Mg II h and k and especially in the short wavelength region, were very weak. Similarly the background signal was set as far as possible away from the source signal without running into the neighbouring orders. An additional complication was present for Ly α because of contamination due to the geocoronal emission. Flux calibrations were incorporated using the data of Bohlin and Holm (1981) and Cassatella et al. (1981). It should be noted that fluxes below 1250 Å are somewhat uncertain.

3. Evidence for photospheric spots

3.1. Spot modelling

The light curve for II Peg during the third quarter of 1984 is given in Fig. 1. At least two minima are apparent from the light curve, corresponding to meridian passage of at least two centres of spot activity. A Fourier fit was made to obtain an initial estimate of the phases of these minima for input into the spot modelling program.

Spot modelling of the light curve was performed using interactive and batch FORTRAN programs written by one of us (PBB), which are based on the single-spot formulation of Friedemann and Gurtler (1975) but adapted for two (or more) circular spots. The parameters of the spot models were stellar inclination, the ratio of spot temperature to that of the stellar photosphere, the star's unspotted magnitude, coefficient of limb darkening, the spot radii and the latitudes of their centres as well as the phases of maximum spot visibility. As the spot modelling is highly non-unique, it is necessary to constrain the fits as far as possible.

The factor that most affects the size of the spots is the unspotted magnitude of the star, V_0, viz. the brighter V_0 the larger the spots have to be to obtain the required depths of the light curve minima. Previous modelling has adopted a number of different values for the unspotted magnitude of II Peg. Chugainov (1976) observed $V_{max} \approx 7.18$. Vogt (1980) and Poe and Eaton (1985) argued that, since no other observer recorded $V \leqq 7.35$, that this is $V_{unspotted}$ and that Chugainov's V_{max} resulted from a zero-point error. A re-examination of Chugainov's data does not support this hypothesis (Chugainov, private communication). Furthermore, recent observations give $V_{max} \approx 7.30$ (Byrne, 1986; Doyle et al., 1987).

The raises a fundamental problem with the process of spot modelling optical light curves. Since $V_{unspotted}$ in this case is at least $\Delta V = 0.15$ greater than the observed maximum light, we require that there be spots in view at all phases covering a sufficient surface area to depress the light output by that amount. We have no knowledge from the observed light curve as to how these spots are distributed. For example, we could claim with equal validity that the spots are distributed in a band about the equator of the star or that there is a large polar spot, which, being at the pole, would be visible at all phases. The latter approach is the one adopted in Paper I while other authors have adopted the former approach (Bopp and Noah, 1980b). In this paper we will model only the degree of asymmetry in the spot distribution required to account for the observed modulation and simply note the additional spot area required to depress the light maximum.

As II Peg is a single line spectroscopic binary the inclination is indeterminate. We have followed the procedure of Paper I and made separate models using inclinations of 55° and 30°. The temperature difference, ΔT, between spot and photosphere was set to 1200 K, a typical value from previous modelling. We would remark here that the choice of ΔT is not critical since changes of a hundred degrees only changes the contrast between spot and photosphere by only a few percent. The coefficients of limb-darkening for the spotted and unspotted portions of the star were assumed the same and taken from the tables of Kopal (1959).

The latitudes of the individual spots are not well constrained by the modelling procedure. Therefore we have imposed the condition that they be at such a latitude that they cross the stellar meridian as close as possible to the observer's line-of-sight. This should result in a minimal area solution.

The resulting fits to the observed light curve are given in Fig. 1 and Table 3. Note that the spot area required to depress the light curve maximum from $V_{unspotted} = 7.30$ is equivalent to a single circular spot of radius $R = 24°$ on the meridian at all phases. Such

Table 3. Spot radii (R_1, R_2) and latitudes (Lat_1, Lat_2) derived from two-spot modelling from the photometry discussed here (1984), in Paper IX (1983), and in Paper I (1981). i is the inclination of II Peg's rotational axis with respect to the line-of-sight while φ_1 and φ_2 are the phases of meridian crossing of the two spots

Year	i	R_1	Lat_1	$\varphi_{1\,min}$	R_2	Lat_2	$\varphi_{2\,min}$
1984	55°	21°	35°	0.88	21°	07°	0.25
1983	55°	19°	40°	0.74	13°	37°	0.25
1981	55°	25°	40°	0.78	16°	37°	0.50
1984	30°	18°	48°	0.88	14°	65°	0.25
1983	30°	22°	62°	0.23	13°	53°	0.80
1981	30°	30°	62°	0.80	16°	53°	0.49

Table 4. Equivalent widths (EW) of the TiO bands as a function of phase

λλ	Equivalent width (mÅ)			
	$\varphi=0.26$	$\varphi=0.41$	$\varphi=0.56$	$\varphi=0.71$
6171.17–76.09	282	406	369	–
6345.14–54.46	407	487	426	–
Sub-total EW	689	893	795	–
6509.42–14.79	193	208	92	189
6651.59–57.39	236	303	255	191
Sub-total EW	429	511	347	380
6718.36–20.01	119	135	129	–
6724.48–30.77	403	435	416	–
6800.27–11.50	588	717	561	–
6814.21–25.32	607	851	765	–
Sub-total EW	1717	2138	1871	–
Total EW	2835	3602	3013	–

a spot would occupy ≈10% of the star's surface area. Adopting Chugainov's $V_{\text{unspotted}}=7.18$ increases this to $R=31°$, corresponding to ≈15% of the stellar surface. These areas are additional to those given in the table.

3.2. Variation of mean photospheric temperature from TiO band strengths

The starspot hypothesis would suggest that the mean surface temperature of a spotted star should be lower at light curve minimum than at maximum. Our $(V-I)_{\text{KC}}$ colour curve (Fig. 1) indicates that this is indeed the case. The broadband colour effect is small however and so it is interesting to see if there exists a spectral signature of the cool spots in II Peg's photospheric spectrum. A sensitive temperature indicator for temperatures cooler than II Peg's spectral type is the strengths of the molecular TiO bands. Vogt (1981) demonstrated, by comparing a spectrum of II Peg taken at photometric maximum and one taken at minimum, that there was a change in the strengths of TiO bands in the sense that the bands were relatively stronger (greater equivalent width) at light curve minimum.

We have examined our spectra in the vicinity of a number of TiO band heads for evidence of changes in equivalent width with phase. Because the TiO bands are relatively weak features and the underlying K2 spectrum has a high density of atomic lines, caution was exercised in selecting those bands which were relatively free from contamination by other strong lines. An obvious difficulty in determining equivalent widths in the spectra was in defining the continuum level in a consistent way. The adopted procedure was to identify, for each band under consideration, the highest features on either side which were common to all nights' observations and then defining a qualitative continuum level using these features as reference markers.

The wavelengths of the bands used and their "equivalent widths" determined in this way are presented in Table 4. The sum total of the individual TiO band "equivalent widths" are plotted as a function of phase in the bottom panel of Fig. 1.

4. Variation of chromospheric/transition region line flux with spot visibility

4.1. Optical emission lines

The final columns of the upper section of Table 2 give the fluxes, above a locally defined continuum level, of each of the visible region emission lines. In determining these line fluxes it is important to define the continuum in a consistent way from one spectrum to another. This was done by taking the mean of a large number of the highest points in each spectral region, which are common to all the nightly spectra. The line flux was determined both by representing the line profiles by gaussians and by direct summation of the flux in each pixel within the line. There is uncertainty in both these procedures. In the first case, while gaussians represented the Ca II profiles well, they were not as good in the case of Hα. On the other hand, the pixel summation method has no objective way of determining the limits of the lines. Nevertheless the two methods gave agreement to a few percent which seemed acceptable. The figures given in the Table 2 are those for the pixel summations.

4.2. The Mg II h and k lines

The final columns of the lower part of Table 2 give the IUE emission line fluxes determined in a similar manner. Defining the background continuum is not as severe a problem in the case of these lines since it is relatively weak. The Mg II h and k lines were represented by a pair of gaussians, one for the main stellar component, the other for the narrow absorption component, which we consider to be interstellar in origin (see Paper III for a discussion on this point). The continuum is represented by a linear fit and the interstellar component is assumed to be unresolved, and so was fixed in width at the instrumental width. The resulting two-gaussian fits yield a constant wavelength for the absorption component to better than 0.01 Å. Best fit parameters are presented in Table 5. Flux entries in Table 2 are corrected for this absorption feature. There also appears to be a slight blue wing excess over and above our fits on the spectrum at $\varphi\approx0.64$. Figure 3 shows the Mg II k profiles and the fits made to them.

4.3. The Ly α line

The Ly α profile is more complicated, having three components, viz. the stellar component, one for the geocoronal emission and an absorption component which is interstellar in origin. Initially, the spectra were shifted so that the geocoronal emission was centred on its rest wavelength of 1215.59 Å (Giddings, 1983b). The geocoronal emission fills the spectrograph slit uniformly and its profile is therefore a three-fold convolution of the projected shape of the spectrograph slit, the scanning slit and the instrumental profile. The flux from the geocorona is an additive flux and we chose to fit it separately using the instrumental details given in Bianchi et al. (1981).

The combined stellar-interstellar Ly α profile was modelled by convolving a Gaussian profile, representing the stellar component, with a naturally broadened profile representing the interstellar absorption. The core of the intrinsic stellar profile is essentially unknown, as the interstellar absorption removes a large part of the core of the line. The interstellar line centre was fixed at the rest wavelength of 1215.67 Å, consistent with the near-zero Mg II h and k interstellar velocity determined above, and the stellar line centre was set at the wavelength determined from the

Table 5. Mg II k, Ca K, Ly α and Hα line fit parameters. $\Delta\lambda$ is the line width (FWHM), N_{HI} the interstellar hydrogen column density and λ_c the line centre. v_{abs} and v_{em} are the velocities, relative to the photospheric rest frame, of the absorption reversal and emission feature referred to in Sect. 7.4

Line	φ	Origin	$\Delta\lambda$ (Å)	N_H (10^{18} cm^{-2})	λ_c (Å)	v_{abs} (km s^{-1})	v_{em} (km s^{-1})
Mg II k	0.197	Stellar	0.87	–	2795.61		
Mg II k	0.197	Interstellar	0.19[a]	–	2795.47		
Mg II k	0.642	Stellar	0.86	–	2794.91		
Mg II k	0.642	Interstellar	0.19[a]	–	2795.47		
Ca II K	0.251	Stellar	0.65	–	3933.56		
Ca II K	0.398	Stellar	0.59	–	3933.26		
Ca II K	0.554	Stellar	0.59	–	3932.81		
Ca II K	0.705	Stellar	0.59	–	3932.55		
Ly α	0.218	Stellar	1.4	–	1215.45		
Ly α	0.218	Interstellar	–	1.0	1215.37		
Ly α	0.664	Stellar	1.1	–	1215.12		
Ly α	0.664	Interstellar	–	0.9	1215.37		
Hα	0.256	Stellar	2.13	–	6562.59	− 4	+ 5
Hα	0.401	Stellar	1.90	–	6561.96	0	+11
Hα	0.557	Stellar	1.98	–	6561.31	+12	+21
Hα	0.707	Stellar	2.24	–	6560.91	+24	+32

[a] The width of the interstellar Mg II feature has been fixed at this value

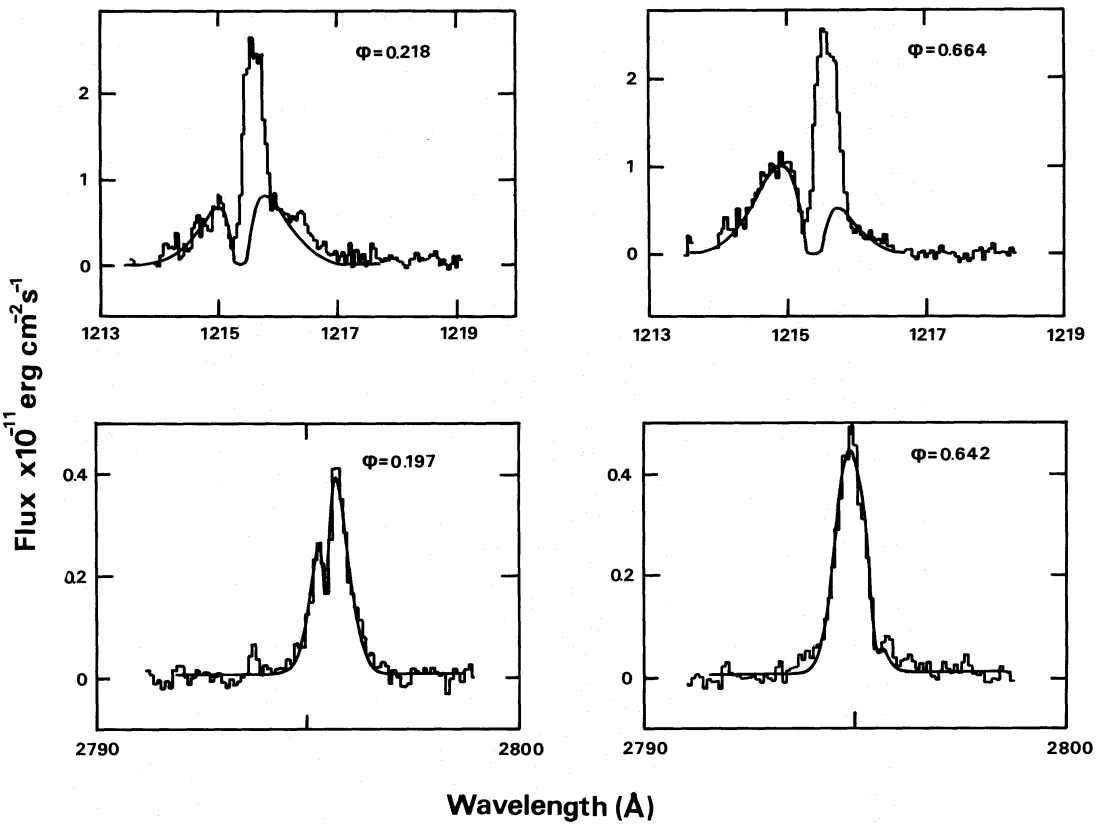

Fig. 3. Ly α (upper panels) and Mg II k (lower panels) line profiles derived from the IUE spectra. The solid curves are gaussian fits to these. The Ly α fits are to the stellar and interstellar components only (see text for details)

radial velocity curve (Vogt, 1981). The free parameters of the fits were the stellar profile width and intensity, and the interstellar profile width which is a measure of the hydrogen column density. The adopted procedure was to fit the blue wing of the stellar line profile and the blue edge of the interstellar absorption dip, which are free of geocoronal emission in both spectra. Using this approach we found that it was not possible to fit both wings of the combined profile by this method. This was true even though the total interstellar hydrogen column densities determined from the two spectra were consistent to within 10% at 1 10^{18} cm^{-2}. As a result we were forced to the conclusion that the stellar emission is not symmetric about the stellar radial velocity.

The derived hydrogen column density corresponds, at a distance of 30 pc (Paper I), to a mean line-of-sight density of $n_{\rm H\,I} \approx 0.01$ cm^{-3}. Recent determinations of $n_{\rm H\,I}$ in the local interstellar medium point to values in the range $0.005 - 0.01$ cm^{-3} (Bruhweiler and Kondo, 1982; Innes and Hartquist, 1984), in good agreement with our result. The Ly α flux entries in Table 2 are corrected for both geocoronal emission and the interstellar absorption, but assume a gaussian profile for the stellar profile. Figure 3 shows the profiles and the adopted fits. Best fit parameters are presented in Table 5.

4.4. *The other UV lines*

The derivation of the remaining UV line fluxes (i.e. those of O I ($\lambda\lambda$1302/5/6 Å), C II ($\lambda\lambda$1335/6 Å), C IV ($\lambda\lambda$1548/51 Å), He II (λ1640 Å) and Si II ($\lambda\lambda$1808/17/18 Å)) also deserves some special mention. All of these lines are weakly exposed on our spectra and background extraction and removal of noise spikes presented special problems. The entire procedure was repeated several times and by different people to try to minimize subjectivity. Some of these lines were particularly affected by noise and for this reason their fluxes are not given in Table 2. For instance, the entire O I ($\lambda\lambda$1302/5/6 Å) multiplet and the C IV (λ1550 Å) line could not be extracted from the first SWP spectrum because of locally severe background noise, while the C II (λ1335 Å) line was affected by cosmic ray hits. It is difficult to place an estimate on the uncertainty due to the extraction procedure but this could be as high as $\pm$30% for the λ1548 Å component of the C IV line and $\pm$20% for the He II line. The profiles of two examples lines and the fits made to them will be found in Fig. 4. Note that we have indicated the contribution made by a cosmic ray activated pixel by a dashed line.

5. Emission line profiles

5.1. *Optical emission lines*

The profiles of the Ca II H and K lines and of Hε along with the gaussian fits made to them on the first of the four nights of observation will be found in Fig. 2. The Hα line on all four nights will also be found in Fig. 2 along with least squares gaussian fits. The parameters of these fits are given in Table 5. It will be noticed that gaussians fit the Ca II profiles very well with the FWHM almost constant apart from a slightly, but significantly, greater width of the first night. There is no clear evidence for asymmetries or variation in profile with phase.

The situation with Hα is quite different however. Gaussians are not an adequate fit to the profile on any of the four nights. At first sight there appears to be a central reversal to the emission profile, whose strength and position relative to the line centroid is

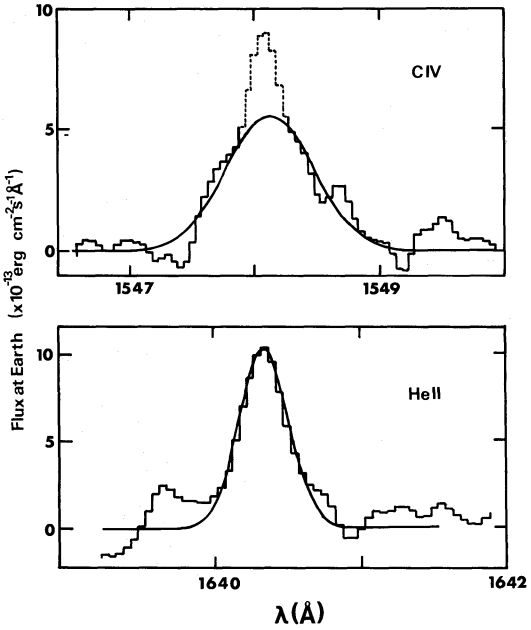

Fig. 4. C IV λ1548 Å and He II line profiles (histogram) and the least squares gaussian fits made to them (continuous curve). The dashed portion of the C IV line illustrates the effect of the cosmic ray activated pixel mentioned in the text

different from night to night. In addition there is a gross asymmetry to the line in the sense of a skewness to the blue which becomes progressively more marked as we progress through the sequence. With this variation in the profile it is difficult to define the line FWHM in a consistent way. Nevertheless there is clearly a variation whatever definition is adopted, in the sense that the first night's profile is the broadest.

5.2. *UV emission lines*

Table 6 gives the widths (FWHM) of the various emission lines in the IUE SWP wavelength range. These have been derived by fitting gaussian functions to the line profiles. Examples of the fits achieved are given in Fig. 4. The accompanying error estimates are the formal errors of the gaussian fits, evaluated by a method of least squares. Also listed in this table are the expected Doppler plus instrumental widths derived from the temperature of formation of the relevant ion. It will immediately be seen that the observed widths greatly exceed the Doppler plus instrumental widths, an effect previously noted on other active stars (Ayres et al., 1983; Elgaroy et al., 1988). More careful perusal of Table 6 however also shows that the excess of observed FWHM over Doppler increases with temperature of formation of the ion. This effect was also noted by Elgaroy et al. in the dMe star, AT Mic. There does not appear to be any significant difference in widths between the two spectra.

6. The orbit of II Peg

Radial velocities were determined from the Doppler shifts of the nightly optical spectra. Approximately seventy photospheric absorption lines were used, arising mainly from neutral iron and iron peak elements and neutral calcium. The majority of lines used came from the 200 Å region centred on the Ca II H and K lines. Line identifications were made with the aid of the line lists of

Table 6. Gaussian widths (FWHM) of UV emission lines. The figures in brackets are the FWHM in km s^{-1}. An entry thus (–) indicates that the line was unmeasurable

	log T	FWHM (Å) (km s^{-1})		Instr.+Doppler FWHM (Å) (km s^{-1})
		$\varphi=0.218$	$\varphi=0.664$	
O I ($\lambda\lambda$1302/5/6 Å)	–[a]	–	0.4±0.1 (90)	–
Si II ($\lambda\lambda$1808/16.7 Å)	4.1	0.3±0.1 (50)	0.3±0.1 (50)	0.12 (20)
C II ($\lambda\lambda$1335/6 Å)	4.3	0.4±0.2 (90)	0.5±0.1 (110)	0.10 (22)
He II (λ1640 Å)	4.7	0.4±0.1 (70)	0.5±0.2 (90)	0.17 (31)
C IV ($\lambda\lambda$1548/51 Å)	5.0	0.8±0.2 (150)	0.8±0.2 (150)	0.15 (29)

[a] O I is pumped by Lyβ and so is not formed in thermal equilibrium

Table 7. Heliocentric radial velocities determined from optical and Mg II k line spectra. Φ are phases from Raveendran et al. (1981). v_{obs} is our observed radial velocity, v_V is the radial velocity at the corresponding phases predicted by Vogt's ephemeris and v_R are those given by the ephemeris of Raveendran et al.

Φ	v_{obs} (km s^{-1})	v_V	v_R
Mean radial velocities from optical lines			
0.555	−40.98±4.45	−40.98	−30.71
0.705	−57.26±7.15	−54.51	−53.70
0.251	15.43±2.80	16.81	19.71
0.398	− 8.22±4.97	− 6.98	4.37
Mean radial velocities from Mg II k line			
0.642	−60.05	−52.44	−47.04
0.197	15.01	19.03	17.79

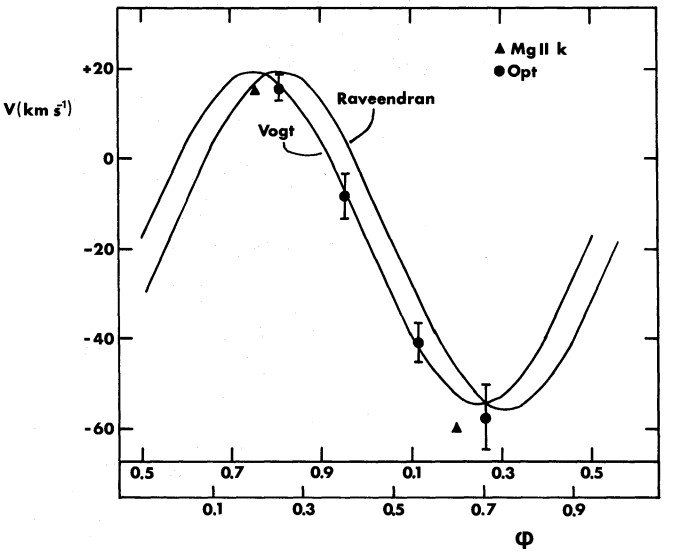

Fig. 5. Heliocentric radial velocity curves at the mean epoch of our present observations as derived from the ephemerides of Vogt (1981) (upper scale) and Raveendran et al. (1981) (lower scale). The radial velocities derived from the Mg II k emission lines and the optical absorption lines in the present data are also plotted

Davis (1947) and Mackle et al. (1975), for the giants β Peg and α Boo respectively, and the MIT wavelength tables (Harrison, 1969). As the nightly spectra varied in both profile and amplitude, caution was exercised in selecting the narrowest, least blended lines with well determined centres. Gaussian profiles were fitted to the lines for a more accurate determination of central wavelength. The statistical mean of these radial velocities is presented in Table 7 along with the velocities predicted by the ephemerides of Vogt (1981) and Raveendran et al. (1981). All velocities are heliocentric.

Radial velocities were also determined from the IUE LWR spectra, using the Mg II k line profiles. The magnesium radial velocities were determined relative to the interstellar absorption component present in the profile. The velocity determined from the spectrum at $\varphi \approx 0.64$ is subject to a larger fitting error in that the absorption component lies in the red wing of the stellar component. Therefore the latter radial velocity is biased to the blue. These radial velocities are also listed in Table 7.

In Fig. 5 we compare the observed points with the radial velocity curves of Raveendran et al. and Vogt. It is quite evident that Vogt's curve agrees much better with our data. It is worth remarking that both the Mg II points lie below the Vogt curve, the point at $\varphi \approx 0.64$ being further removed than that at $\varphi \approx 0.20$ for the reason given in the last paragraph. The deviation of the point at $\varphi \approx 0.20$ is consistent with a small negative radial velocity for the interstellar Mg II in the direction of II Peg of the order of -5 km s^{-1}.

7. Discussion

7.1. Comparison of emission line fluxes with those observed previously

We first of all compare our derived emission line fluxes with those derived by other authors. In Paper III we observed IUE short

wavelength line fluxes from II Peg at two discrete levels of emission. These we termed "active" and "quiescent", even though the implied "quiescent" surface fluxes are orders of magnitude greater than the quiet Sun. The average Mg II k, C IV and He II fluxes derived here (38.7, 7.7, and 3.6 10^{-13} erg cm^{-2} s^{-1} respectively) are comparable to, but somewhat less than, the "quiescent" levels previously recorded (50.6, 9.5, and 4.5 10^{-13} erg cm^{-2} s^{-1} in 1981 (Paper III) and 63.2, 8.6, and 5.5 10^{-13} erg cm^{-2} s^{-1} in 1983 (Paper IX)). It should be noted though that there is considerable intrinsic scatter in the individual fluxes, particularly those for C IV and He II, and some values previously observed are as low as those recorded here.

Ramsey and Nations (1984) reported Hα equivalent widths for II Peg taken during 1981. Their observations were made at a mixture of resolutions, one data set being at $\approx$1 Å resolution, the other at $\approx$0.5 Å. These two datasets overlap in time and yet there is a systematic difference in the flux [expressed as equivalent widths (EW)] between the two. While this may be due to real variability, it may also be due to the difficulty in setting the continuum levels adequately, a difficulty which is exacerbated when observing at lower resolutions. Nevertheless we have compared our EW's with theirs. They find values from -0.07 Å (i.e. net absorption) to 1.94 Å. These may be compared with ours which range from 0.69 Å to 1.39 Å. Bopp and Noah (1980a) also observed II Peg at Hα in 1978 but at a resolution of $\approx$0.3 Å. They also found a large scatter in EW from $\approx$0.2 Å to $\approx$2.0 Å with a tendency to cluster in phase.

More recently Liu and Tan (1987) observed II Peg at Hα in late November/early December 1984 again at a resolution of $\approx$0.3 Å. They find, on five consecutive nights, monotonically decreasing EW's from 1.22 Å to 0.64 Å. Three weeks later a single observation yields a value of 0.86 Å. This range of values agrees excellently with ours. This is encouraging since these data are closest to ours in time ($\approx$140 days later). Huenemoerder and Ramsey (1987) also observed II Peg at Hα twice in December 1984 at a resolution of $\approx$0.5 Å. Unfortunately their equivalent widths are for the difference between II Peg and an Hα absorption line star ε Eri, rather than the emission flux above the local continuum as given here. As well as we can determine from their data as published, their emission line fluxes agree well with ours.

We have been unable to find previously published values of either the Ca II H and K or Ly α fluxes in II Peg, so a comparison here is not available. Nevertheless the Ca II line surface fluxes are typical of those found in other RS CVn stars (Fernandez-Figueroa et al., 1986).

7.2. *Evidence for rotational modulation*

What of evidence for rotational modulation of II Peg's emission lines? Comparison of Tables 2 and 5 and Fig. 1 shows that the observed fluxes in the Ca II doublet, Hα, Hε, C IV and He II are at a maximum around the phase of maximum spottedness ($\varphi \approx 0.25$–0.3) i.e. minimum of the V light curve. This is suggestive of a correlation between the optical spot and overlying emission from the chromosphere to the transition region. Matters are not so simple, however, as the Mg II flux is greater at earlier phase. Furthermore the Hα flux does not vary smoothly with spot phase, showing a recovery at phase $\varphi = 0.56$. By way of contrast the Ca II flux declines monotonically from close to the phase of maximum spot visibility to near minimum spottedness. This lack of agreement between the Ca II and Mg II fluxes is especially puzzling since these two lines are formed in a very similar temperature regime in the atmosphere. It is possible that we have underestimated the contribution of the interstellar Mg II absorption, however its contribution is too small to account for the discrepancy. We must bear in mind however that the IUE and INT spectra were not simultaneous. Thus it is possible that a temporary, flare-like brightening affected the optical emission lines which was not present at the time of the ultraviolet observations, 8.5 h earlier.

More recently Huenemoerder (1987) has shown that II Peg has stronger TiO band strengths at all phases than a standard star of the same spectral type which otherwise shows a good spectral match.

7.3. *Widths of Ca II K and Mg II k emission*

The Wilson-Bappu relationship is a well-established, empirical relationship between the width of the Ca II features in cool stars and their absolute V magnitude. Giampapa et al. (1979) concluded, from a survey of Ca II K in the magnetically active dMe stars, that they obey the Wilson-Bappu relationship as amended by Lutz (1970). (Lutz showed that the original subjective width of the original relationship was identical to the FWHM of the emission core.) We compare the observed FWHM for the Ca II K line with that derived from the Lutz expression i.e., taking II Peg's unspotted V magnitude as $V \approx 7.2$ and its distance as 30 pc, we derive $W_0 \approx 33$ km s^{-1}. This compares with our observed values ranging from 45–50 km s^{-1}.

Weiler and Oegerle (1979) have shown that there exists a similar relationship between the base width of the Mg II emission lines and absolute V magnitude, M_V. Ayres et al. (1983) and Elgaroy et al. (1988) have demonstrated that this relationship may also be extended to the active dMe stars. We have compared the width of our Mg II k line profiles with the relationship of Weiler and Oegerle and again find that the widths are much too great. The full width of the k line at base on the spectrum at $\varphi = 0.197$ (i.e. the spectrum where the base width is least affected by interstellar absorption) is $W_{\mathrm{Mg\,k}} \approx 280$ km s^{-1}. This may be compared to that predicted by the Weiler and Oegerle relation i.e. $W_{\mathrm{Mg\,k}} \approx 100$ km s^{-1}.

Glebocki and Stawikowski (1978) noted that there was an intensity dependence in the Wilson-Bappu effect for Ca II K in the sense that, the more intense the emission, the more the star deviated from the mean relationship in the direction of being intrinsically too bright. This effect could be in excess of two magnitudes in M_V. Bielicz et al. (1985) attempted to account for these effects in terms of the effects of rotation on the line profiles. They modelled the Ca II K and Mg II k lines for a range of temperatures and gravities. Their model which lies closest to II Peg ($\log g = 3.0$ and $v \sin i = 20$ km s^{-1}) gives an excess broadening of 0.34 Å over a non-rotating star, very similar to that observed on II Peg. Unfortunately, their modelling of Mg II k profiles indicates that this line is affected *less* than Ca II K by rapid rotation, the inverse of what we see on II Peg.

Ayres (1979), on the other hand, has derived a parametrized Wilson-Bappu relationship using scaling laws for the thickness and mean electron density of stellar chromospheres in terms of $\log g$ and the rate of non-radiative heating. His expression for the width of the line involves terms for the rate of non-radiative heating and for turbulent broadening due to velocity fields. Unfortunately, his heating parameter is not directly related to the observed quantities except through detailed modelling. We note however that the chromospheric heating rates of the RS CVn and dMe stars, as derived from radiative cooling rates, are similar ($\approx 10^5$–10^6 erg cm^{-2} s^{-1}) (see e.g. Paper III). So it seems improb-

able that the heating rate term in Ayres relationships can account for the deviation.

We are left, therefore, with the possibility of broadening due to turbulence. We have presented evidence in Sect. 5.2 above for excess broadening in the mid-transition region of the order of 150 km s^{-1}. If turbulent motions on this scale apply also to the chromosphere of II Peg, then a substantial part of the deviation from the Wilson-Bappu type relationships may be explainable.

7.4. *Profiles of higher temperature lines*

How do we interpret the excess broadening of the high temperature lines and the dependence of this effect on temperature? Rotational broadening for II Peg is $\approx$21 km s^{-1} (Vogt, 1981), which is insufficient to account for the discrepancy, even in the coolest lines. Turbulent motion on a global scale appears to be required. Brueckner and Bartoe (1983) have observed short-lived "turbulent events" and higher velocity "jets" of material on the Sun at C IV temperatures. The former show a velocity range of $\pm$75–140 km s^{-1} and a global solar birth rate of $\approx$750 s^{-1}. The "jets" occur at a much lower rate ($\approx$24 s^{-1}) and are directed rather than turbulent, with velocities of up to $\approx$400 km s^{-1}. These appear to be present even on the quiet Sun and may be associated with the heating of the solar corona. A similar phenomenon on II Peg could account for the observed effect but would require that these events occur at a variety of temperature levels, from the upper chromosphere to the mid-transition region. On the Sun they have been detected at temperatures down to Si III (λ1206 Å) (log $T_e \approx 4.3$).

Referring back to the width of the Mg II k line and its excess over the predictions of the Wilson-Bappu type relationship of Weiler and Oegerle, we may perhaps invoke a similar extra broadening mechanism in the chromosphere to account for it too.

7.5. *Profiles of Hα and Lyα*

We have remarked in Sect. 5.1 above on the asymmetry in the Hα profile. It is most symmetric on the first night of observation just before light minimum and when the dominant spot group is close to meridian passage. It then becomes increasingly asymmetric in the sense that the blue peak is higher than the red. Furthermore the position of the central absorption reversal also appears to vary in a systematic way from night to night. This can be interpreted either as the passage of absorbing material across the disk of the star or, equally, as an emission feature being carried by the rotation of the star. The measured velocities of both the absorption and emission features relative to the photosphere are given in Table 5. The velocity amplitudes over the three day interval are 28 km s^{-1} for the absorption and 27 km s^{-1} for the emission features, respectively. These should be compared with the measured $v \sin i$ of $\approx$21 km s^{-1} (Vogt, 1981).

To illustrate these ideas we have plotted in Fig. 6 the optical spectra in the immediate vicinity of Hα but having scaled the peak flux in each profile to that of the first in the sequence. Note that the spectra have been shifted to the rest frame of the photospheric absorption spectrum. The proposed emission feature is arrowed on all four spectra. It will be noted that it is least well defined on the first night's spectrum.

Previous authors have remarked on the dramatic variability of the Hα profile in II Peg (see e.g. Bopp and Noah, 1980a; Nations and Ramsey, 1980; Vogt, 1981; Huenemoerder and Ramsey, 1987). The most extensive of these were the observations of Vogt. He remarks on the redward asymmetry of the Hα profile, a result

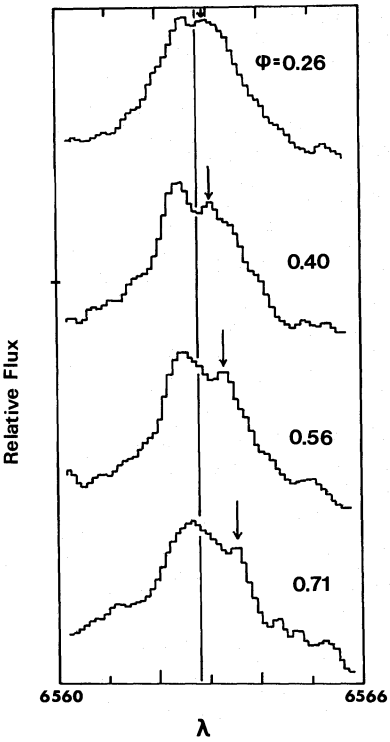

Fig. 6. Hα emission profiles on the four nights of observation in the rest frame of the primary, with peak flux scaled to that of the first night. The vertical line is the rest wavelength of Hα. The arrowed feature is discussed in the text (Sect. 7.5)

confirmed here, and the presence of an absorption feature near the peak of the emission. Unlike our central reversal, his remained fixed as a function of phase at close to the rest wavelength. It is variable, however, and like ours, it is most pronounced when the line itself is weakest.

How can we interpret these Hα data? It is clear that there is a velocity effect in the line profile which is too large to be due to any uncertainties in our velocity scale ($\approx$5 km s^{-1}, see Table 7). The velocity amplitude of the effect is appreciably less than the total velocity amplitude across the stellar disk. If this feature were due to a discrete region on the surface of II Peg then, whether it is an absorption or an emission feature, the symmetry of its velocity about the photospheric velocity requires that there be internal downflow within the region of order 10–20 km s^{-1}. Such velocities have been observed in the Mg II lines on II Peg (Doyle et al., 1989) and on V711 Tau (Linsky et al., 1988, Paper X in this series) but during flares. The velocity amplitude of the feature over the three day interval would correspond to a latitude of $\pm$45°. Comparison with the spot modelling in Table 3 shows that one of the major spot groups is at a comparable latitude. However, the phase relationship with the spot groups is not direct. From the mid-point of the velocity variation the suggested feature would transit mid-disk at about $\varphi \approx 0.5$, i.e. at a phase intermediate between the two major spots. Carrying this picture further, this would suggest a plage (emission) or dark prominence (absorption) lying in a position between the main spot groups.

The Lyα profiles also exhibit an asymmetry about the mean stellar velocity as discussed in Sect. 4.3. In this case however the detected excess emission is also to the red (see Fig. 3) but is more pronounced at the earlier phase ($\varphi \approx 0.22$). Our observations of Lyα are too sparse however to discuss this point further, except to remark that red asymmetry appears to occur in Lyα as for Hα.

7.6. *Radiative losses from II Peg*

We note here that the major source of chromospheric radiative loss, in any one line, is Ly α. This is in contrast to the observations by Baliunas et al. (1984) of the RS CVn star λ And, in which Mg II and Ca II emission dominate Ly α. They do not correct for interstellar absorption in Ly α, however.

By taking a straight mean, we find the sum of the observed chromospheric line fluxes excluding Ly α (i.e. $F(\text{Ca II}) + F(\text{Mg II}) + F(\text{H}\alpha) + F(\text{H}\varepsilon)$) is $1.76\ 10^{-11}$ erg cm^{-2} s^{-1} at Earth, compared to $1.64\ 10^{-11}$ erg cm^{-2} s^{-1} for Ly α alone. It is clear that Ly α is a major source of chromospheric radiative losses from II Peg. The total transition region losses in the temperature range $4.3 \leqq \log T_e \leqq 5.4$, derived using the emission measure curves of Byrne et al. (1987) and Doyle et al. (1988) scaled to the mid-transition region fluxes derived here are $\approx 2.2\ 10^{-11}$ erg cm^{-2} s^{-1}. Thus discussion of the energy balance of stellar chromospheres without taking Ly α into account are in serious danger of giving false results.

Correcting the observed total chromospheric emission to radiative losses at the star assuming a distance of 30 pc (Paper III) yields a value of $6.0\ 10^{30}$ erg s^{-1}. Correction for the unobserved members of the Lyman and Balmer series is unknown but it does not seem likely to be more than a factor of two or three. Thus the total chromospheric radiative losses from II Peg at the star are ≈ 1–$2\ 10^{31}$ erg s^{-1}. This is comparable to the coronal soft X-ray flux (0.26–3 keV) observed by Walter et al. (1980) of about $4\ 10^{31}$ erg s^{-1} and the hard X-ray flux (2–10 keV) observed by Schwarz et al. (1981) of about $5\ 10^{30}$ erg s^{-1}.

We note that Bruner and McWhirter (1988) have derived a relationship between the flux of a single mid-transition region line, such as C IV (λ 1548 Å), and the total radiative losses from the entire outer atmosphere, between $4.0 \leqq \log T_e \leqq 8.0$. Doyle et al. (1988) have demonstrated that this may be applied to active stellar atmospheres with some success. Applying it to the C IV (λ 1548 Å) line flux in Table 2 yields $2.6\ 10^{31}$ erg s^{-1}, within a factor of 1.5 of the observed total losses derived by adding the losses quoted above. This result would suggest that the shape of the emission measure curve on II Peg are similar to the Sun.

8. Conclusions

We have presented high-resolution ultraviolet and optical spectroscopy, as well as optical broadband photometry, of the RS CVn star II Peg during a 4-day interval in mid-1984. It provides evidence of changes in the distribution of brightness in the photosphere, chromosphere and transition region. Furthermore, the data suggest that these changes are interliked in such a way as to point to rotation as the root cause. Downflows of order 10–20 km s^{-1} appear to be present throughout the chromosphere, even in its quiescent (non-flaring) state. Evidence of turbulence, probably on a global scale, and exhibiting a range of velocity which increases with temperature (up to ≈140 km s^{-1}) has been derived. We point to a possible counterpart to this phenomenon in the solar transition region.

II Peg does not obey the basic Wilson-Bappu relation nor the similar Weiler-Oegerle relation for Mg II emission line width. We suggest that the excess broadening may also have its origins in turbulence at chromospheric level.

Changes in the equivalent width of TiO bands are consistent with the cool spot hypothesis for explaining the observed modulation of visible light. The relationship between changes in TiO band strength and the V light curve is not straightforward however.

The radiative energy balance of the outer atmosphere of II Peg has been derived and Lα shown to be a very important component.

Acknowledgements. We are grateful to Dr. J.V. Wall of the Royal Greenwich Observatory for carrying out the optical observations and to the ground staff at the European IUE ground station at Vilspa, Madrid for their help in making the ultraviolet observations. We also acknowledge permission to use spectroscopic data provided by the NASA World Data Centre at the Goddard Space Flight Centre, Maryland, USA. J. Linsky and J. Neff (JILA) made very useful comments on an early draft of this paper.

References

Andrews, A.D., Butler, C.J., Linsky, J.L., Brown, A., Rodonò, M., Catalano, S., Scaltriti, F., Busso, M.: 1988, (Paper IX) *Astron. Astrophys.* **204**, 177
Arevalo, M.J., Lazaro, C., Fuensalida, J.J.: 1985, *IAU Comm. 27, Inf. Bull. Var. Stars*, No. 2840
Ayres, T.R.: 1979, *Astrophys. J.* **228**, 509
Ayres, T.R., Eriksson, K., Linsky, J.L., Stencel, R.E.: 1983, *Astrophys. J.* **270**, L17
Baliunas, S.L., Guinan, E.F., Dupree, A.D.: 1984, *Astrophys. J.* **282**, 733
Bianchi, L., Northover, K., Clavell, J.: 1981, *IUE VILSPA user's guide*, Vol. II, p. 20
Bielicz, E., Glebocki, R., Sikorski, J.: 1985, *Astron. Astrophys.* **153**, 269
Bohlin, R.C., Holm, A.V.: 1981, *NASA IUE Newsletter*, No. 10, 37
Bopp, B.W., Noah, P.V.: 1980a, *Publ. Astron. Soc. Pacific* **92**, 333
Bopp, B.W., Noah, P.V.: 1980b, *Publ. Astron. Soc. Pacific* **92**, 717
Bromage, G.E.: 1984, *Proc. Fourth. European IUE Conference*, ESA SP-218, p. 473
Brueckner, G.E., Bartoe, J.-D.F.: 1983, *Astrophys. J.* **272**, 329
Bruhweiler, F.C., Kondo, Y.: 1982, *Astrophys. J.* **259**, 232
Bruner, M.E., McWhirter, R.W.P.: 1988, *Astrophys. J.* **326**, 1002
Byrne, P.B.: 1986, *Inf. Bull. Var. Stars*, No. 2951
Byrne, P.B., Doyle, J.G., Brown, A., Linsky, J.L., Rodonò, M.: 1987, *Astron. Astrophys.* **180**, 172 (Paper VI)
Cassatella, A., Ponz, D., Selvelli, P.L.: 1981, *ESA IUE Newsletter* No. 10, 31
Chugainov, P.F.: 1976, *Izv. Krymskoi Astron. Obs.* **54**, 89
Davis, D.N.: 1947, *Astrophys. J.* **106**, 28
Doyle, J.G., Byrne, P.B., van den Oord, G.H.J.: 1989, *Astron. Astrophys.* (in press)
Doyle, J.G., Butler, C.J., Morrison, L.V., Gibbs, P.: 1987, *Astron. Astrophys.* **192**, 275
Elgaroy, O., Joras, P., Engvold, O., Jensen, E., Pettersen, B.R., Ayres, T.R., Ambruster, C., Linsky, J.L., Clark, M., Marang, F.: 1988, *Astron. Astrophys.* **193**, 211
Fernandez-Figueroa, M.J., Montesinos, B., de Castro, E., Rego, M., Gimenez, A., Reglero, V.: 1986, *Astron. Astrophys.* **169**, 219
Friedemann, C., Gurtler, J.: 1975, *Astron. Nachr.* **296**, 125
Giampapa, M.S., Worden, S.P., Schneeberger, T.J., Cram, L.E.: 1979, *Astrophys. J.* **246**, 502
Giddings, J.: 1983a, *IUE ESA Newsletter*, No. 17, p. 53
Giddings, J.: 1983b, *IUEDR User Guide*, Version 1.2
Glebocki, R., Stawikowski, A.: 1978, *Astron. Astrophys.* **78**, 69

Harrison, G.R.: 1969, *Massachussetts Institute of Technology Wavelength Tables*, MIT Press
Howarth, I.D., Masdlen, D.E.: 1983, *STARLINK User Notes*, No. 50
Huenemoerder, D.P.: 1987, *Proc. 5th Cambridge Workshop on Cool Stars*, eds. J.L. Linsky, R.E. Stencel. Springer, Berlin, Heidelberg, New York, p. 512
Huenemoerder, D.P., Ramsey, L.W.: 1987, *Astrophys. J.* **319**, 392
Innes, D.E., Hartquist, T.W.: 1984, *Monthly Notices Roy. Astron. Soc.* **209**, 7
Kaluzny, J.: 1984, *Inf. Bull. Var. Stars*, No. 2627
Kopal, Z.: 1959, Close Binary Systems, Chapman and Hall, London
Linsky, J.L., Neff, J.E., Brown, A., Gross, B.D., Simon, T., Andrews, A.D., Rodonò, M., Feldman, P.A.: 1988, *Astron. Astrophys.* (in press)
Liu, X-f., Tan, H-s.: 1987, *Chin. Astron. Astrophys.* **11**, 64
Lutz, T.E.: 1970, *Astron. J.* **75**, 1007
Mackle, R., Griffin, R., Holweger, H.: 1975, *Astron. Astrophys. Suppl.* **19**, 303
Menzies, J.W., Banfield, R.M., Laing, J.D.: 1980, *SAAO Circular* **1**, 149
Poe, C.H., Eaton, J.A.: 1985, *Astrophys. J.* **289**, 644
Ramsey, L.W., Nations, H.L.: 1984, *Astron. J.* **89**, 115
Raveendran, A.V., Mohin, S., Mekkaden, M.V.: 1981, *Monthly Notices Roy. Astron. Soc.* **196**, 299
Rodonò, M.: 1986, *Cool Stars, Stellar Systems and the Sun*, Proc. 4th Cambridge Workshop on Cool Stars, eds. M. Zeilik, D.M. Gibson, Springer, Berlin, Heidelberg, New York, p. 475
Rodonò, M., Cutispoto, G., Pazzani, V., Catalano, S., Byrne, P.B., Doyle, J.G., Butler, C.J., Andrews, A.D., Blanco, C., Marilli, F., Linsky, J.L., Scaltriti, F., Busso, M., Cellino, A., Hopkins, J.L., Akazaki, A., Hayashi, S.S., Zeilik, M., Helston, R., Henson, G., Smith, P., Simon, T.: 1986, *Astron. Astrophys.* **165**, 135 (Paper I)
Rodonò, M., Byrne, P.B., Neff, J.E., Linsky, J.L., Simon, T., Butler, C.J., Catalano, S., Cutispoto, G., Doyle, J.G., Andrews, A.D., Gibson, D.M.: 1987, *Astron. Astrophys.* **176**, 267 (Paper I)
Schwartz, D.A., Garcia, M., Ralph, E., Doxsey, R.E., Johnston, M.D., Lawrence, A., McHardy, I.M., Pye, J.P.: 1981, *Monthly Notices Roy. Astron. Soc.* **196**, 95
Vogt, S.S.: 1980, *Astrophys. J.* **240**, 567
Vogt, S.S.: 1981, *Astrophys. J.* **247**, 975
Vogt, S.S.: 1983, in *Activity in Red Dwarf Stars, Proc. IAU Coll.* **71**, eds. P.B. Byrne, M. Rodonò, Reidel, Dordrecht, p. 137
Walter, F.M., Cash, W., Charles, P.A., Bowyer, C.S.: 1980, *Astrophys. J.* **236**, 212
Weiler, E.J., Oegerle, W.R.: 1977, *Astrophys. J. Suppl.* **39**, 537